

Atomic Layer Deposition of Metal Oxides on Pristine and Functionalized Graphene

Xinran Wang, Scott M. Tabakman, and Hongjie Dai*

Department of Chemistry and Laboratory for Advanced Materials, Stanford University, Stanford, California 94305

Received March 29, 2008; E-mail: hdai@stanford.edu

Graphene has recently emerged as an interesting material for electronics due to extremely high carrier mobility in bulk graphene¹ and the demonstration of all-semiconducting sub-10-nm graphene nanoribbons.² Aggressive device scaling requires integration of ultrathin high- κ dielectrics in order to achieve high on-state current and ideal subthreshold swing without substantial gate leakage.³ Deposition of metal oxides including high- κ dielectrics on graphene has not been systematically investigated thus far. Uniform oxide deposition on graphene by atomic layer deposition (ALD) is expected to be difficult due to the lack of dangling bonds in the graphene plane, as in the case of the carbon nanotube.^{4,5} As a result, previously reported topgated graphene devices used very thick (≥ 15 nm) ALD dielectrics on top of a negative tone resist⁶ or functional layer⁷ to prevent gate leakage. Functionalization is likely needed for uniform ALD on graphene.

Here we show that ALD of metal oxides gives no direct deposition on defect-free pristine graphene. On the edges and defect sites, however, dangling bonds or functional groups can react with ALD precursors to afford active oxide growth. This leads to an interesting and simple way to decorate and visualize defects in graphene. By noncovalent functionalization of graphene with carboxylate-terminated perylene molecules, one can coat graphene with densely packed polar groups for uniform ALD of high- κ dielectrics. Uniform high- κ coverage is achieved on large pieces of graphene sheets with a size of greater than $5\ \mu\text{m}$. This method opens the possibility of integrating ultrathin high- κ dielectrics in future graphene electronics.

Our graphene sheets were obtained by standard peel-off method on 300 nm SiO_2/Si substrate described in ref 8. We first identified few-layer (≤ 5 layers) graphene sheets under an optical microscope. Then the chip was annealed at $600\ ^\circ\text{C}$ in vacuum with 1 Torr argon atmosphere to clean the substrate and graphene sheets, followed by atomic force microscopy (AFM) imaging of the few-layer graphene sheets. Then the chip was soaked in 3,4,9,10-perylene tetracarboxylic acid (PTCA) solution for ~ 30 min, thoroughly rinsed, and blown dry (see Supporting Information). The chip was immediately moved into the ALD chamber to prevent contamination by molecules in the air. We then deposited Al_2O_3 at $\sim 100\ ^\circ\text{C}$ using trimethylaluminum and water as precursors.⁹ In the same run, we also included a SiO_2/Si chip covered by PMMA except for some prepatterned squares to measure Al_2O_3 thickness (see Supporting Information).

We first carried out the study on pristine graphene. Figure 1a,b shows AFM images of the same area before and after ALD of ~ 2 nm Al_2O_3 . Before ALD, the height of the triangular graphene piece at the bottom and the large piece on the left was ~ 1.7 and ~ 2.0 nm, respectively. Near the edge of the 2.0 nm graphene, there was also a narrow ~ 1.0 nm high stripe. After ALD, ~ 2.0 nm Al_2O_3 was coated on SiO_2 ; the apparent topography height of the three graphene sheets was obviously reduced to a level similar to that of the ALD-coated SiO_2 . The height difference before and after ALD indicates no Al_2O_3 coating on pristine graphene sheets. This is because ALD relies on chemisorption or rapid reaction of precursor molecules with surface functional groups.^{5,10} Since pristine graphene does not have any

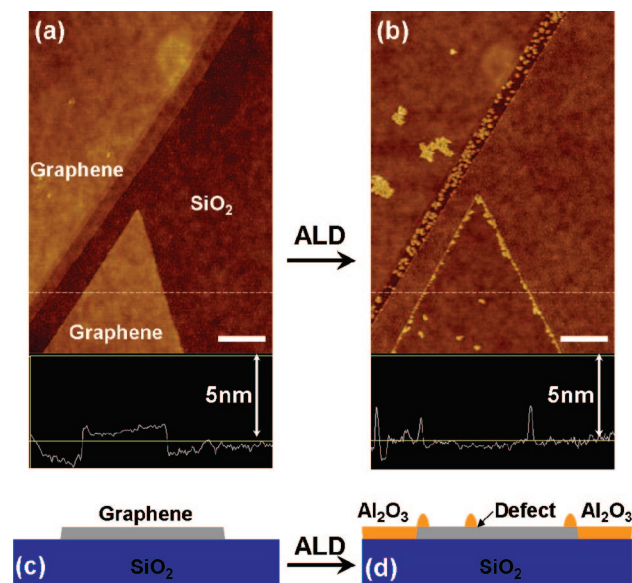


Figure 1. ALD of Al_2O_3 on pristine graphene. (a) AFM image of graphene on SiO_2 before ALD. The height of the triangular shaped graphene is ~ 1.7 nm as shown in the height profile along the dashed line cut. Scale bar is 200 nm. (b) AFM image of the same area as (a) after ~ 2 nm Al_2O_3 ALD deposition. The height of the triangular shaped graphene becomes ~ 0.3 nm as shown in the height profile along the dashed line cut. Scale bar is 200 nm. (c) and (d) Schematics of graphene on SiO_2 before and after ALD. The Al_2O_3 grows preferentially on graphene edge and defect sites.

dangling bonds or surface groups to react with precursors, no ALD occurs on the graphene plane. Interestingly, we observed quasi-continuous bright lines of Al_2O_3 preferentially grown on the edges of graphene sheets, suggesting dangling bonds on the edges or possible termination by $-\text{OH}$ or other reactive species (Figure 3b). We also observed some bright dots in the middle of graphene sheets, likely corresponding to defects such as pentagon–hexagon pairs or vacancies known to exist in graphite¹¹ (Figure 3c). Thus, our ALD method could be used as a novel way to probe and visualize defects in graphene, which is much simpler and more efficient than current STM¹² and TEM¹¹ measurements. The peeled off graphene sheets could be defect-free for a few micrometers, as evidenced by AFM images after ALD (see Supporting Information). However, defects do exist in the graphene planes and should be considered in other studies.

In order to afford uniform ALD coating on pristine graphene, functionalization of graphene is needed to induce uniform surface groups as active ALD nucleation sites. PTCA is an excellent candidate for selective coating of graphitic surfaces on the SiO_2/Si substrate owing to its planar, conjugated ring system and its symmetrically arranged, negatively charged terminal carboxylates (Figure 3). While PTCA noncovalently partitions and adheres to graphene, likely via π – π stacking and hydrophobic forces,^{13,14} basic conditions deprotonate the terminal acid groups, yielding a tetra-anionic state which is

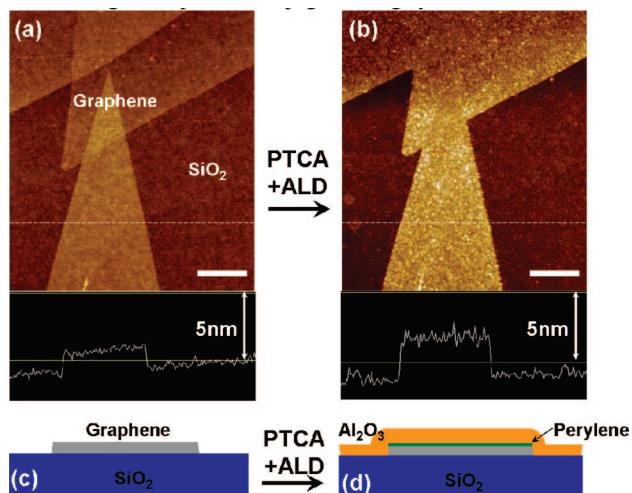


Figure 2. ALD of Al_2O_3 on PTCA-coated graphene. (a) AFM image of graphene on SiO_2 before ALD. The height of the triangular shaped graphene is ~ 1.6 nm as shown in the height profile along the dashed line cut. Scale bar is 500 nm. (b) AFM image of the same area as (a) after ~ 2 nm Al_2O_3 ALD deposition. The height of the triangular shaped graphene becomes ~ 3.0 nm as shown in the height profile along the dashed line cut. Scale bar is 500 nm. (c) and (d) Schematics of graphene on SiO_2 before and after ALD. The Al_2O_3 grows uniformly on noncovalently PTCA-coated graphene.

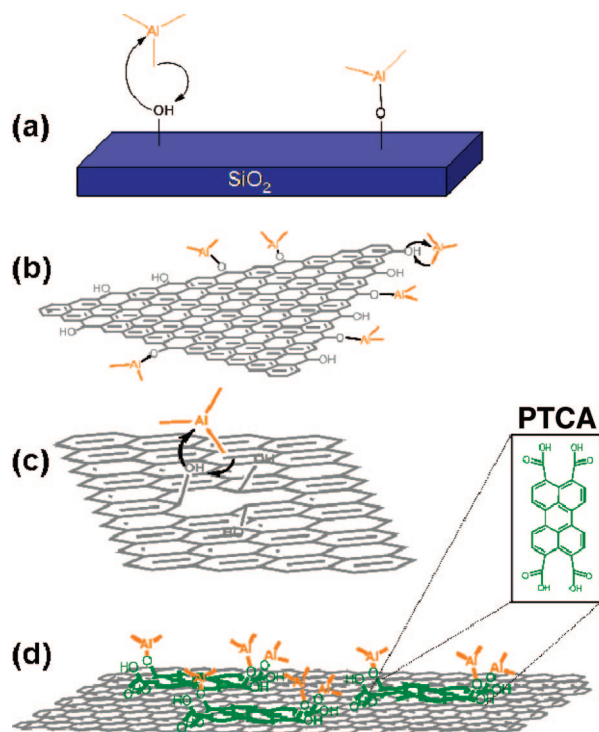


Figure 3. Schematics of atomic layer deposition of aluminum oxide via trimethylaluminum (TMA) precursor on (a) bare SiO_2 substrate, (b) a single-layer graphene sheet with edges, (c) graphene containing a defect site, and (d) perylene tetracarboxylic acid (PTCA)-coated graphene. PTCA selectively adheres to graphene on SiO_2 surfaces, providing binding sites for TMA deposition. Inset is a top view of PTCA structure.

repulsed from the oxidized silica surface. Following adsorption onto graphitic surfaces, the carboxylate functional groups on the perylene moiety serve as uniformly distributed sites for nucleation of ALD (Figure 3d).

Figure 2a,b shows AFM images of the same area for PTCA-treated sample before and after ~ 2 nm Al_2O_3 deposition. Before ALD, the

graphene under the line cut was ~ 1.6 nm high, while after ALD, the height increased to ~ 3.0 nm as shown in the height profile in Figure 2b. The relative height increase of Al_2O_3 -coated graphene was partly attributed to the thickness of PTCA layer, which was usually ~ 0.5 – 0.8 nm as observed by AFM after PTCA coating step (see Supporting Information). The actual Al_2O_3 on graphene was $\sim 2.8 \pm 0.2$ nm thick in Figure 2b. Complete and uniform PTCA packing is evidenced by Al_2O_3 coated over the whole piece of graphene, which is several micrometers in size. The mean roughness of the Al_2O_3 film on graphene is ~ 0.33 nm over a $2.5 \mu\text{m} \times 2.5 \mu\text{m}$ area as measured with several pieces (see Supporting Information). Previous high-vacuum STM studies have confirmed two modes of epitaxial packing of the PTCA precursor, perylene tetracarboxylic dianhydride, along the lattice lines of highly oriented pyrolytic graphite.^{13,14} As the partitioning of PTCA from methanol to the graphene interface should be highly favorable, it is likely that similar epitaxial packing is occurring in the solution phase, yielding dense, uniform coating of graphene sheets. This self-assembly process of PTCA on graphene is responsible for uniform Al_2O_3 film coating. Note that noncovalent functionalization for ALD is not expected to degrade the electrical properties of graphene, similar to the case of single-walled carbon nanotubes.⁴

In summary, we found that ALD of metal oxide cannot directly be deposited on pristine graphene without surface functionalization due to the lack of dangling bonds and surface functional groups. ALD could grow actively on edge and defect sites of graphene, which could be used as a simple and effective probe to defects. We used carboxylate-terminated perylene molecules to functionalize graphene with densely packed functional groups and achieved uniform ultrathin Al_2O_3 deposition on graphene over a few micrometers. The noncovalent functionalization method is not destructive to graphene and could be used for depositing ultrathin high- κ dielectrics for future graphene electronics.

Acknowledgment. This work was supported by Intel and MARCO MSD Focus Center.

Supporting Information Available: ALD process details, measurement of ALD height using prepatterned PMMA windows, Al_2O_3 film surface roughness, and process of making PTCA solution are described. This material is available free of charge via the Internet at <http://pubs.acs.org>.

References

- (1) Geim, A. K.; Novoselov, K. S. *Nat. Mater.* **2007**, *6*, 183.
- (2) Li, X.; Wang, X.; Zhang, L.; Lee, S.; Dai, H. *Science* **2008**, *319*, 1229.
- (3) Wang, X.; Ouyang, Y.; Li, X.; Wang, H.; Guo, J.; Dai, H. *Phys. Rev. Lett.* **2008**, *100*, 206803.
- (4) Lu, Y.; Bangsaruntip, S.; Wang, X.; Zhang, L.; Nishi, Y.; Dai, H. *J. Am. Chem. Soc.* **2006**, *128*, 3519.
- (5) Farmer, D. B.; Gordon, R. G. *Nano Lett.* **2006**, *6*, 699.
- (6) Ozyilmaz, B.; Jarillo-Herrero, P.; Efetov, D.; Kim, P. *Appl. Phys. Lett.* **2007**, *91*, 192107.
- (7) Williams, J. R.; DiCarlo, L.; Marcus, C. M. *Science* **2007**, *317*, 638.
- (8) Novoselov, K. S.; Jiang, D.; Schedin, F.; Booth, T. J.; Khotkevich, V. V.; Morozov, S. V.; Geim, A. K. *Proc. Natl. Acad. Sci. U.S.A.* **2005**, *102*, 10451.
- (9) Groner, M. D.; Fabreguette, F. H.; Elam, J. W.; George, S. M. *Chem. Mater.* **2004**, *16*, 639.
- (10) Leskela, M.; Ritala, M. *Thin Solid Films* **2002**, *409*, 138.
- (11) Hashimoto, A.; Suenaga, K.; Gloter, A.; Urita, K.; Iijima, S. *Nature* **2004**, *430*, 870.
- (12) Rutter, G. M.; Crain, J. N.; Guisinger, N. P.; Li, T.; First, P. N.; Stroscio, J. A. *Science* **2007**, *317*, 219.
- (13) Hoshino, A.; Isoda, S.; Kurata, H.; Kobayashi, T. *J. Appl. Phys.* **1994**, *76*, 4113.
- (14) Ostrick, J. R.; Dodabalapur, A.; Torsi, L.; Lovinger, A. J.; Kwock, E. W.; Miller, T. M.; Galvin, M.; Berggren, M.; Katz, H. E. *J. Appl. Phys.* **1997**, *81*, 6804.

JA8023059